

A Mutual Coupling Resilient Algorithm for Joint Angle and Delay Estimation

Ahmad Bazzi*[†], Dirk T.M. Sloek*, and Lisa Meilhac[†]

*EURECOM Mobile Communications Department, 450 route des Chappes, 06410 Biot Sophia Antipolis, France
Email: {bazzi,sloek}@eurecom.fr

[†]CEVA-RivieraWaves, 400, avenue Roumanille Les Bureaux, Bt 6, 06410 Biot Sophia Antipolis, France
Email: {ahmad.bazzi, lisa.meilhac}@ceva-dsp.com

Abstract—The problem of Joint Angle and Delay Estimation (JADE) in the presence of mutual coupling is addressed. The system consists of a Single Input Multiple Output (SIMO) link in an OFDM communication setting. This paper presents two resilient algorithms that could cope with mutual coupling. The first one is an extension of an existing algorithm in order to perform JADE, which allows resolvability of more signals. The second algorithm is an improvement of the first one, in the sense that it could handle more mutual coupling parameters. Simulation results show the difference between both algorithms. In addition, the algorithms are compared with the 2D-MUSIC method that performs JADE in the absence of mutual coupling, i.e. when a "coupling-free" model is assumed.

Index Terms—Joint Estimation, Angle-of-Arrival, Time-of-Arrival, Resilient Mutual Coupling, OFDM

I. INTRODUCTION

Mutual coupling between antennas is a popular problem in array signal processing. This phenomenon arises when antennas are close to each other [1], and thus the current developed in an antenna element depends on its own excitation and on the contributions from adjacent antennas. As a consequence, an ideal model is no longer valid, and therefore the performance of the high resolution algorithms that perform Angle-of-Arrival (AoA) estimation, such as MUSIC [2], ESPRIT [3], etc., deteriorate significantly.

Methods that aim on solving the mutual coupling problem are sometimes referred to as calibration methods, which are of two types: Offline and Online. In an offline calibration approach, one estimates the mutual coupling parameters using known locations, such as the techniques in [4]–[6]. In contrast, online calibration consists of jointly estimating the coupling and AoA parameters. Herein, we focus on the latter.

In the literature, several techniques deal with the online calibration problem, such as those found in [7]–[17] and references within. The authors in [7] jointly estimate the coupling parameters and AoAs by alternating minimization steps between the former and the latter using the MUSIC cost function. In [8], the algorithm is iterative and the sources are assumed to be totally uncorrelated. Moreover, the method in [8] estimates the coupling parameters in order to utilize it in the MUSIC cost function. In [9], [10], the array elements are assumed to be partly calibrated. In other words, one has access to a few coupling parameters. Moreover, methods in [13]–[15] propose to use the "middle sub-array". In particular, let N be the number of antennas placed in a uniform and linear fashion, and p be the number of coupling parameters. If $p \leq \frac{N}{2}$, then there exists a "middle sub-array", of size $N - 2p + 2$, over which the effect of the mutual coupling is preserved the *Vandermonde* structure of the array response [13]–[15]. As a matter of fact, one could mathematically show that the array response on the "middle sub-array" is a known functional *Vandermonde* vector multiplied by an unknown scalar, and therefore high resolution techniques could be applied to estimate the AoAs.

However, this is highly suboptimal because only an effective number of antennas, i.e. $N - 2p + 2$, are utilized for parameter estimation. To address this major loss of antennas, the authors in [17] suggest to add "Guard" antennas on the edges of the array, in particular $p - 1$ antennas on the left edge and the other $p - 1$ on the right edge. Therefore, the main array of size N plays the role of a "middle sub-array". The aforementioned argument on the "middle sub-array" holds on the main array. Unfortunately, appending antennas is not possible in some applications, such as Wi-Fi.

Joint Angle and Delay Estimation, also known as JADE, was introduced in [26]. One motivation behind JADE is to increase the number of resolvable signals by transmitting known signals. As a result, this allows estimating signal parameters (AoA/ToA) of a number of signals beyond the number of antennas, thanks to temporal (or frequency, in the case of OFDM) diversity. We outline two contributions of this paper: The first one is an extension to an existing resilient mutual coupling algorithm in order to perform JADE in the presence of mutual coupling. Analogously to the motivation of JADE, this algorithm could handle more coupling parameters, as compared to AoA-only estimation. The second contribution is an improvement of the first algorithm. In particular, the first algorithm requires $p \leq \frac{N}{2}$ to function properly, whereas the second algorithm does not.

Notations: Upper-case and lower-case boldface letters denote matrices and vectors, respectively. $(\cdot)^T$, $(\cdot)^*$, and $(\cdot)^H$ represent the transpose, conjugate, and transpose-conjugate operators. The matrix \mathbf{I} is the identity matrix of suitable dimensions. The operator $E\{\mathbf{X}\}$ returns the expectation of a random matrix \mathbf{X} . For any matrix \mathbf{B} , the operator $\|\mathbf{B}\|_2$ is the *Frobenius* norm.

II. SYSTEM MODEL

A. Mathematical Formulation

Consider an OFDM symbol composed of M subcarriers and centered at a carrier frequency f_c , impinging an array of N antennas via q sources, each arriving at different AoAs $\Theta = \{\theta_1 \dots \theta_q\}$ and ToAs $\mathbf{T} = \{\tau_1 \dots \tau_q\}$. Note that the order in both sets should be respected. In frequency domain, we could express the signal at the n^{th} antenna and m^{th} subcarrier of the l^{th} OFDM symbol as follows [19]:

$$X_{m,n}(l) = b_m \sum_{i=1}^q \gamma_i(l) \tilde{a}_n(\theta_i) e^{-j2\pi m \Delta_f \tau_i} + N_{m,n}(l) \quad (1)$$

with $l = 1 \dots L$, $m = 1 \dots M$, and $n = 1 \dots N$. Moreover, $T = \frac{1}{\Delta_f}$ is the OFDM symbol duration, Δ_f is the subcarrier spacing, b_m is the modulated symbol onto the m^{th} subcarrier, $\tilde{a}_n(\theta)$ is the n^{th} antenna response to an incoming signal at angle θ . Moreover, $\gamma_i(l)$ is the complex coefficient of the i^{th} source during the l^{th} OFDM symbol. The term $N_{m,n}(l)$ is background noise.

We claim that the transmitted OFDM symbol is a preamble field of the Wi-Fi 802.11 frame, thus prior knowledge of the modulated symbols $\{b_m\}_{m=0}^{M-1}$ is a valid assumption. Therefore, we compensate for all such symbols (multiplying by $\frac{b_m^*}{|b_m|^2}$) and hence omit b_m from (1). Re-writing (1) in a compact matrix form, we have:

$$\mathbf{x}(l) = \mathbf{H}\boldsymbol{\gamma}(l) + \mathbf{n}(l) \quad (2)$$

where $\mathbf{x}(l)$ and $\mathbf{n}(l)$ are $MN \times 1$ vectors

$$\mathbf{x}(l) = [X_{1,1}(l) \dots X_{1,N}(l) \dots X_{M,1}(l) \dots X_{M,N}(l)]^T \quad (3)$$

The noise vector $\mathbf{n}(l)$ is defined in a similar manner. The vector $\boldsymbol{\gamma}(l) \in \mathbb{C}^{q \times 1}$ is given as

$$\boldsymbol{\gamma}(l) = [\gamma_1(l) \dots \gamma_q(l)]^T \quad (4)$$

\mathbf{H} is an $MN \times q$ matrix given as

$$\mathbf{H} = [\mathbf{c}(\tau_1) \otimes \tilde{\mathbf{a}}(\theta_1) \dots \mathbf{c}(\tau_q) \otimes \tilde{\mathbf{a}}(\theta_q)] \quad (5)$$

where

$$\mathbf{c}(\tau) = [1, z_\tau \dots z_\tau^{M-1}]^T \quad \text{with} \quad z_\tau = e^{-j2\pi\tau\Delta f} \quad (6)$$

and $\tilde{\mathbf{a}}(\theta)$ is the response of a Uniform Linear Array (ULA) suffering from mutual coupling. Following [11], the response $\tilde{\mathbf{a}}(\theta)$ could be modelled as

$$\tilde{\mathbf{a}}(\theta) = \mathcal{T}_p(\mathbf{m})\mathbf{a}(\theta) \quad (7)$$

where $\mathcal{T}_p(\mathbf{m}) \in \mathbb{C}^{N \times N}$ is a banded symmetric Toeplitz matrix defined as follows

$$\mathcal{T}_p(\mathbf{m}) = \begin{bmatrix} 1 & m_1 & m_2 & \dots & m_{p-1} & 0 & \dots & 0 \\ m_1 & 1 & m_1 & \dots & m_{p-2} & m_{p-1} & \dots & 0 \\ \vdots & & & \ddots & \ddots & & & \vdots \\ 0 & \dots & m_{p-1} & m_{p-2} & \dots & m_1 & 1 & m_1 \\ 0 & \dots & 0 & m_{p-1} & \dots & m_2 & m_1 & 1 \end{bmatrix} \quad (8)$$

and

$$\mathbf{a}(\theta) = [1, z_\theta \dots z_\theta^{N-1}]^T \quad \text{with} \quad z_\theta = e^{-j2\pi\frac{d}{\lambda}\sin(\theta)} \quad (9)$$

where d is the inter-element spacing and λ is the signal's wavelength. The model in equations (7) and (8) suggest that antennas that are placed at least p inter-element spacings apart do not interfere, i.e. $m_i = 0$ for all $i \geq p$. This is due to the fact that the mutual coupling is inversely proportional to the distance between antennas.

B. Assumptions and Problem Statement

Throughout the paper, we assume the following:

- **A1:** \mathbf{H} is full column rank.
- **A2:** The complex coefficients $\boldsymbol{\gamma}(l)$ are fixed within a snapshot, and are uncorrelated over OFDM symbols.
- **A3:** The number of sources, i.e. q , is known.
- **A4:** The vector $\mathbf{n}(l)$ is additive Gaussian noise with zero mean and covariance $\sigma^2\mathbf{I}$ independent from the sources.

The conditions so that assumption **A1** is satisfied are given in [20]. Moreover, if assumption **A2** were not satisfied, i.e. when the sources are a result of multipath propagation, then one could preprocess OFDM symbols by applying Frequency Smoothing¹, which is a 1D version of [21]. For the sake of compactness, we shall assume that the sources are uncorrelated. Furthermore, algorithms exist for

¹Note that one could apply the technique of spatial smoothing [18] over frequencies (i.e. frequency smoothing) since the VanderMonde structure is preserved over the vector $\mathbf{c}(\tau)$ even though mutual coupling is present. For simplicity and due to lack of space, we shall assume uncorrelation of sources.

estimating the number of sources, such as Minimum Description Length [22], Modified MDL [23], Benjamin Hochberg procedure [24], and so forth. Therefore, assumption **A3** is reasonable. Any further assumptions will be mentioned. Now, we address our problem: "Given $\{\mathbf{x}(l)\}_{l=1}^L$, p and q , jointly estimate the signal parameters Θ and \mathbf{T} in the presence of mutual coupling."

III. RESILIENT MUTUAL COUPLING ALGORITHM

A. Algorithm 1: Quadratic Program 1

We start by defining the covariance matrix of the received vector $\mathbf{x}(l)$, i.e.

$$\mathbf{R}_{xx} = \mathbb{E}\{\mathbf{x}(l)\mathbf{x}^H(l)\} \quad (10)$$

In practical scenarios, this matrix is computed thru a sample average as follows $\hat{\mathbf{R}}_{xx} = \frac{1}{L}\mathbf{X}\mathbf{X}^H$, where $\mathbf{X} = [\mathbf{x}(1) \dots \mathbf{x}(L)]$. Let $\hat{\lambda}_1 > \hat{\lambda}_2 > \dots > \hat{\lambda}_{MN}$ and $\hat{\mathbf{u}}_1, \hat{\mathbf{u}}_2 \dots \hat{\mathbf{u}}_{MN}$ denote the eigenvalues and their corresponding eigenvectors of $\hat{\mathbf{R}}_{xx}$. Under assumptions **A1**, **A2** and **A4**, one could jointly estimate $\{(\theta_i, \tau_i)\}_{i=1}^q$ by evaluating the peaks of the following 2D-MUSIC cost function [25], [26]

$$(\hat{\theta}_i, \hat{\tau}_i) = \arg \max_{\theta, \tau} \frac{1}{\mathbf{h}^H(\theta, \tau)\hat{\mathbf{U}}_n\hat{\mathbf{U}}_n^H\mathbf{h}(\theta, \tau)} \quad (11)$$

where $\mathbf{h}(\theta, \tau) = \mathbf{c}(\tau) \otimes \tilde{\mathbf{a}}(\theta)$ and $\hat{\mathbf{U}}_n = [\hat{\mathbf{u}}_{q+1} \dots \hat{\mathbf{u}}_{MN}]$ is called the "noise" subspace. The MUSIC cost function exploits the orthogonality between vectors in the signal and noise subspaces [25]. Unfortunately, MUSIC couldn't be directly applied since the functional form of $\tilde{\mathbf{a}}(\theta)$ is unknown. Before we proceed, we find the following useful:

Definition 1: For any vector $\mathbf{a} \in \mathbb{C}^{N \times 1}$ and matrix $\mathbf{A}_p \in \mathbb{C}^{N \times p}$. We say that " \mathbf{a} generates \mathbf{A}_p ", or $\mathbf{A}_p \triangleq \mathcal{G}_p(\mathbf{a})$, if

$$\mathbf{A}_p = [\mathbf{a} \mid \mathbf{S}_1\mathbf{a} \mid \dots \mid \mathbf{S}_{p-1}\mathbf{a}] \quad (12)$$

where $\mathbf{S}_k \in \mathbb{C}^{N \times N}$ is an all-zero matrix except at the k^{th} sub- and super-diagonals, which are set to 1.

Theorem 1: (Commutativity of Symmetric Toeplitz Matrices) Let $\mathbf{m} = [m_0, m_1 \dots m_{p-1}]^T \in \mathbb{C}^{p \times 1}$ and $\mathbf{a} \in \mathbb{C}^{N \times 1}$. Define the corresponding matrix $\mathcal{T}_p(\mathbf{m})$ as in equation (8). Then the following is true for any $1 \leq p \leq N$

$$\mathcal{T}_p(\mathbf{m})\mathbf{a} = \mathbf{A}_p\mathbf{m} \quad (13)$$

where $\mathbf{A}_p = \mathcal{G}_p(\mathbf{a})$. (See **Definition 1**)

Proof: See [7], [27].

Using **Theorem 1**, we have that

$$\tilde{\mathbf{a}}(\theta) = \mathcal{T}_p(\mathbf{m})\mathbf{a}(\theta) = \mathbf{B}(\theta)\mathbf{m} \quad (14)$$

where $\mathbf{B}(\theta) = \mathcal{G}_p(\mathbf{a}(\theta))$. This theorem allows re-writing the denominator of the 2D-MUSIC cost function in equation (11) as follows

$$\begin{aligned} \mathbf{h}^H(\theta, \tau)\hat{\mathbf{U}}_n\hat{\mathbf{U}}_n^H\mathbf{h}(\theta, \tau) &= \left\| \hat{\mathbf{U}}_n^H(\mathbf{c}(\tau) \otimes \tilde{\mathbf{a}}(\theta)) \right\|_2^2 \\ &= \left\| \hat{\mathbf{U}}_n^H(\mathbf{c}(\tau) \otimes \mathbf{B}(\theta))\mathbf{m} \right\|_2^2 \end{aligned} \quad (15)$$

which is quadratic in \mathbf{m} . Now, let

$$\mathbf{S}(\theta, \tau) \triangleq (\mathbf{c}(\tau) \otimes \mathbf{B}(\theta))^H\hat{\mathbf{U}}_n\hat{\mathbf{U}}_n^H(\mathbf{c}(\tau) \otimes \mathbf{B}(\theta)) \quad (16)$$

If we form the following Quadratic Program (QP)

$$\text{(QP1): } \begin{cases} \text{minimize} & \mathbf{t}^H\mathbf{S}(\theta, \tau)\mathbf{t} \\ & \mathbf{t} \in \mathbb{C}^{p \times 1} \\ \text{subject to} & \mathbf{e}_1^T\mathbf{t} = 1 \end{cases} \quad (17)$$

then the solution is the cost function $f_1(\theta, \tau)$ [27], where its q peaks are estimates of the signal parameters $\{(\theta_i, \tau_i)\}_{i=1}^q$:

$$f_1(\theta, \tau) = \mathbf{e}_1^T \mathbf{S}^\dagger(\theta, \tau) \mathbf{e}_1 \quad (18)$$

where the constraint in equation (17) is to exclude the trivial solution. Similar to [27], the identifiability conditions of $f_1(\theta, \tau)$ are:

- **B1:** $q + p \leq MN$
- **B2:** $p \leq \frac{N}{2}$

Condition **B2** is due to the following property:

Property 1: For ULA type configurations, i.e. $\mathbf{a}(\theta) = [1, z_\theta, \dots, z_\theta^{N-1}]^T$ with $z_\theta = e^{-j2\pi \frac{d}{\lambda} \sin(\theta)}$. Define the following sets:

$$\Theta_+ = \{\theta = \sin^{-1}(\frac{k\lambda}{Nd}), k = -\frac{N}{2} \dots \frac{N}{2}\} \quad (19a)$$

and

$$\Theta_- = \{\theta = \sin^{-1}(\frac{(k + \frac{1}{2})\lambda}{Nd}), k = -\frac{N}{2} \dots \frac{N}{2}\} \quad (19b)$$

Also, let $\Theta_\pm = \{\Theta_+ \cup \Theta_-\}$. The matrix $\mathbf{B}(\theta) = \mathcal{G}_p(\mathbf{a}(\theta))$ has the following characteristics:

- Iff $p < \frac{N+2}{2}$, the matrix $\mathbf{B}(\theta)$ is full column rank.
- When $p \geq \frac{N+2}{2}$, there are two cases
 - Iff N is even and $\theta \in \Theta_+$, then $\text{rank}(\mathbf{B}(\theta)) = \frac{N}{2}$. Furthermore, iff N is even and $\theta \in \Theta_-$, then $\text{rank}(\mathbf{B}(\theta)) = \frac{N}{2} + 1$. Otherwise, $\mathbf{B}(\theta)$ is full column rank.
 - Iff N is odd and $\theta \in \Theta_\pm$, then $\text{rank}(\mathbf{B}(\theta)) = \frac{N+1}{2}$. Otherwise, $\mathbf{B}(\theta)$ is full column rank.

Proof: See [28].

B. Algorithm 2: Quadratic Program 2

When assumption **B2** is not satisfied, the function $f_1(\theta, \tau)$ is maximised at $\theta \in \Theta_\pm$ for any τ . This could be seen from the objective function of QP1 in (17): When $\theta \in \Theta_\pm$, then according to **Property 1**, the matrix $\mathbf{B}(\theta)$ admits a null space, therefore the cost function is minimized. To circumvent this issue, we form a new Quadratic Program (QP2), which minimizes the same cost function, but under a different constraint, viz.

$$\text{(QP2): } \begin{cases} \underset{\mathbf{t}}{\text{minimize}} & \mathbf{t}^H \mathbf{S}(\theta, \tau) \mathbf{t} \\ \text{subject to} & \mathbf{e}_1^T \mathbf{B}(\theta) \mathbf{t} = 1 \end{cases} \quad (20)$$

The solution of QP2 is given in [28], which is the following

$$f_2(\theta, \tau) = \mathbf{a}_p^T(\theta) \mathbf{S}^\dagger(\theta, \tau) \mathbf{a}_p^*(\theta) \quad (21)$$

where $\mathbf{a}_p(\theta)$ is a steering vector of a p -sized ULA array, namely $\mathbf{a}_p(\theta) = [1, z_\theta \dots z_\theta^{p-1}]^T$. The ToAs and AoAs are obtained by selecting the q peaks of the $f_2(\theta, \tau)$.

IV. ANALYSIS OF $f_1(\theta, \tau)$ VS $f_2(\theta, \tau)$

In this section, we justify the identifiability conditions of $f_2(\theta, \tau)$, which are given as follows:

- **C1:** $q + p \leq MN$
- **C2:** $p < N$

Condition **C1** is common to $f_1(\theta, \tau)$ and $f_2(\theta, \tau)$. This is due to the fact that the projection matrix onto the noise subspace, i.e. $\hat{\mathbf{U}}_n \hat{\mathbf{U}}_n^H$ is of rank $MN - q$. Furthermore, the dimension of matrix $\mathbf{S}(\theta, \tau)$ is $p \times p$. In order to preserve the rank of the noise subspace projector, we should have $p \leq MN - q$, provided that $\mathbf{B}(\theta)$ is full column rank (i.e. when **B2** is satisfied). This argument justifies the conditions of $f_2(\theta, \tau)$ when **B2** is true. In what follows, we argue the case when $\frac{N}{2} < p < N$.

For the sake of argument and compactness, let us assume true subspaces (i.e. high SNR or number of snapshots), so we shall replace $\hat{\mathbf{U}}_n$ by \mathbf{U}_n . The MUSIC criterion implies that

$$\|\mathbf{U}_n^H(\mathbf{c}(\tau_i) \otimes \mathbf{B}(\theta_i)) \mathbf{t}\|_2^2 = 0, \quad (\theta_i, \tau_i) \in (\Theta, \mathbf{T}) \text{ and } \mathbf{t} = \mathbf{m} \quad (22)$$

Equation (22) along with **Property 1** imply the following

- *Case 1:* The rank of $\mathbf{S}(\theta_i, \tau_i)$ is $p - 1$, if $(\theta_i, \tau_i) \in (\Theta, \mathbf{T})$ and $\theta_i \notin \Theta_\pm$. In addition, the only eigenvector that spans the nullspace of $\mathbf{S}(\theta_i, \tau_i)$ is \mathbf{m} . This is equivalent to equation (22).
- *Case 2:* The rank of $\mathbf{S}(\theta_i, \tau_i)$ is $p - \delta$ if $\theta_i \in \Theta_\pm$ and $\theta_i \notin \Theta$, $\forall \tau_i$, where δ is the dimension of the null space of $\mathbf{B}(\theta_i)$. This is a direct result of **Property 1** when $p \geq \frac{N+2}{2}$.
- *Case 3:* The rank of $\mathbf{S}(\theta_i, \tau_i)$ is $p - \delta - 1$ if $(\theta_i, \tau_i) \in (\Theta, \mathbf{T})$ and $\theta_i \in \Theta_\pm$. It has been proven in [28] that the vector \mathbf{m} is linearly independent from the vectors that form the null space of $\mathbf{B}(\theta_i)$. In other words, $\mathcal{N}(\mathbf{S}(\theta_i, \tau_i)) = \mathcal{N}(\mathbf{B}(\theta_i)) \cup \{\mathbf{m}\}$
- *Case 4:* Otherwise, $\mathbf{S}(\theta_i, \tau_i)$ is full rank.

Let us discuss the first three cases. Using spectral decomposition, we can say

$$\mathbf{S}(\theta_i, \tau_i) = \mathbf{V} \Phi \mathbf{V}^H \quad (23)$$

where the k^{th} column of \mathbf{V} is the k^{th} eigenvector² of $\mathbf{S}(\theta_i, \tau_i)$, denoted as \mathbf{v}_k and its corresponding eigenvalue is the k^{th} smallest eigenvalue found in the k^{th} diagonal entry of Φ , denoted as ν_k . We adopt "diagonal loading" for the pseudo inverse, namely

$$\mathbf{S}^\dagger(\theta_i, \tau_i) = (\mathbf{S}(\theta_i, \tau_i) + \epsilon \mathbf{I})^{-1} = \mathbf{V} \Sigma \mathbf{V}^H \quad (24)$$

where $\Sigma = (\Phi + \epsilon \mathbf{I})^{-1}$. Consider the quadratic function $f(\theta, \tau) = \mathbf{y}^H \mathbf{S}^\dagger(\theta_i, \tau_i) \mathbf{y}$. When $\mathbf{y} = \mathbf{e}_1$, then $f(\theta, \tau) = f_1(\theta, \tau)$ and when $\mathbf{y} = \mathbf{a}_p^*(\theta)$, then $f(\theta, \tau) = f_2(\theta, \tau)$. Furthermore, we can re-write $f(\theta, \tau)$ as follows

$$f(\theta, \tau) = \sum_{k=1}^p \frac{1}{\nu_k + \epsilon} \|\mathbf{y}^H \mathbf{v}_k\|_2^2 \quad (25)$$

Case 1 implies that $\nu_1 = 0$ while $\nu_k > 0$ for all $k \geq 2$. Therefore, $f(\theta_i, \tau_i) \sim \frac{1}{\epsilon} \|\mathbf{y}^H \mathbf{m}\|_2^2 \xrightarrow{\epsilon \rightarrow 0} \infty$, provided that $\|\mathbf{y}^H \mathbf{m}\|_2^2 \neq 0$. It is easy to see that the norm term is not zero if $\mathbf{y} = \mathbf{e}_1$, since the first element of \mathbf{m} can not be zero. As for $\mathbf{y} = \mathbf{a}_p^*(\theta)$, the conditions on \mathbf{m} so that $\|\mathbf{y}^H \mathbf{m}\|_2^2 \neq 0$ should be found in [28]. We conclude that both functions $f_1(\theta, \tau)$ and $f_2(\theta, \tau)$ peak at the true values (θ_i, τ_i) defined in *Case 1*.

Case 2 implies that $\nu_1 = \dots = \nu_\delta = 0$, while $\nu_k > 0$ for all $k \geq \delta + 1$. Therefore,

$$f(\theta_i, \tau_i) \sim \frac{1}{\epsilon} \sum_{k=1}^{\delta} \|\mathbf{y}^H \mathbf{v}_k\|_2^2 \quad (26)$$

When $\mathbf{y} = \mathbf{e}_1$, the norm term is not necessarily zero. Therefore, $f_1(\theta, \tau)$ peaks at values of $\theta_i \in \Theta_\pm$ for any τ_i . However, when $\mathbf{y} = \mathbf{a}_p^*(\theta_i)$, then the norm term is exactly zero because

$$f(\theta_i, \tau_i) \sim \frac{1}{\epsilon} \sum_{k=1}^{\delta} \|\mathbf{a}_p^T(\theta_i) \mathbf{v}_k\|_2^2 = \frac{1}{\epsilon} \sum_{k=1}^{\delta} \|\mathbf{e}_1^T \mathbf{B}(\theta_i) \mathbf{v}_k\|_2^2 = 0 \quad (27)$$

since \mathbf{v}_k span the null space of $\mathbf{B}(\theta_i)$. We conclude that $f_1(\theta, \tau)$ yields fake peaks as explained wherever $f_2(\theta, \tau)$ doesn't.

Using the same reasoning, both functions $f_1(\theta_i, \tau_i)$ and $f_2(\theta_i, \tau_i)$ peak at values given in *Case 3*.

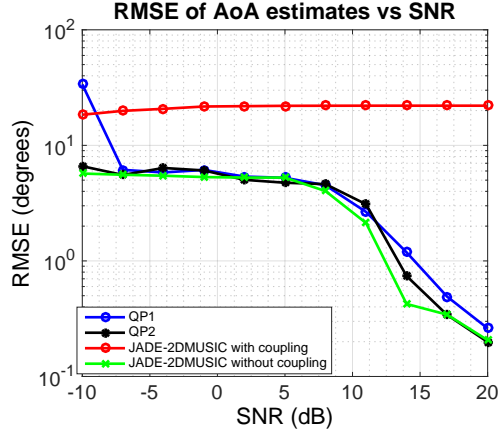


Fig. 1: RMSE of AoAs on a log-scale vs. SNR of the 1st experiment.

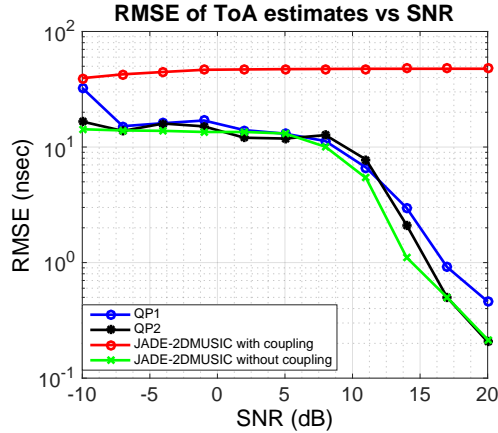


Fig. 2: RMSE of ToAs on a log-scale vs. SNR of the 1st experiment.

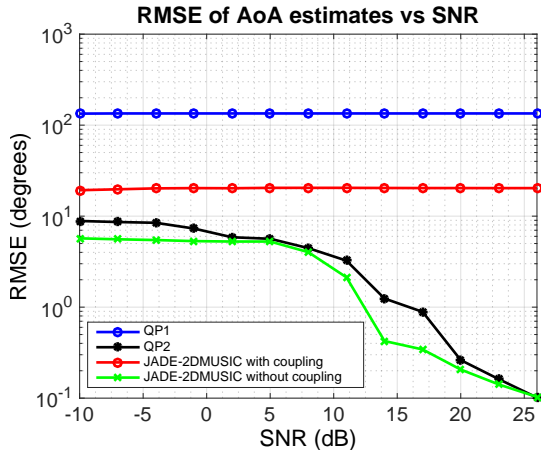


Fig. 3: RMSE of AoAs on a log-scale vs. SNR of the 2nd experiment.

V. SIMULATION RESULTS

In this section, two experiments are conducted. In particular, we are interested in observing the Root-Mean-Squared-Error (RMSE) of

²Indeed, \mathbf{V} and Φ are functions of (θ, τ) .

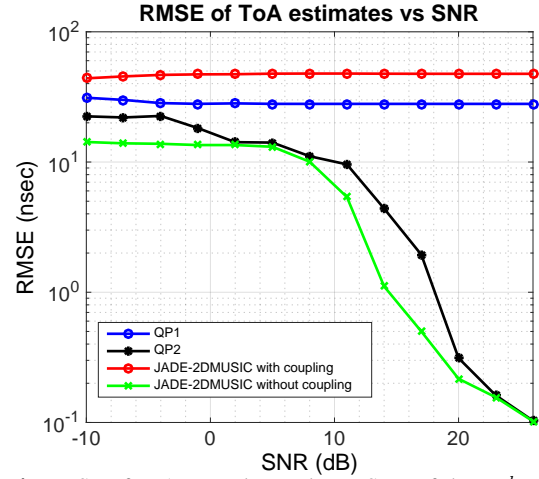


Fig. 4: RMSE of ToAs on a log-scale vs. SNR of the 2nd experiment.

ToAs and AoAs when condition **B2** is respected (1st experiment) and violated (2nd experiment). Note that **C2** is always respected. We fix the following parameters:

- $N = 5$ antennas and $M = 64$ subcarriers.
- $d = \frac{\lambda}{2}$ and $\Delta_f = 312500$ MHz (a total bandwidth of 20 MHz).
- $L = 100$ snapshots and 200 Monte-Carlo simulations.
- $q = 4$ multipaths, with:
 - $\Theta = [-60^\circ, -50^\circ, -40^\circ, -30^\circ]$.
 - $\mathbf{T} = [10 \text{ nsec}, 35 \text{ nsec}, 50 \text{ nsec}, 75 \text{ nsec}]$.
 - $\gamma(l)$ are chosen according to a Gaussian distribution.

In the 1st experiment (Fig. 1 and Fig. 2), the number of coupling parameters is set to $p = 2$ (condition **B2** is respected), and are given as $\mathbf{m} = [1, 0.343 + j0.3638]^T$. Clearly, applying 2D-MUSIC to perform JADE in the presence of mutual coupling gives bad performance. Furthermore, at $-7 \text{ dB} \leq \text{SNR} \leq 10 \text{ dB}$, we can see that the performance of $f_1(\theta, \tau)$ and $f_2(\theta, \tau)$ is close to that of 2D-MUSIC, when applied to a "coupling-free" model. Moreover, we also observe that $f_2(\theta, \tau)$ coincides with the "coupling-free" model, when the SNR exceeds 17 dB. Also, there is a gain of almost 0.1° in terms of AoA (Fig. 1) and 0.3 nsec in terms of ToA (Fig. 2) when compared with $f_1(\theta, \tau)$.

In the 2nd experiment (Fig. 3 and Fig. 4), the number of coupling parameters is set to $p = 4$ (condition **B2** is violated), and are given as $\mathbf{m} = [1, 0.415 - j0.28, -0.224 - j0.246, 0.214 - j0.13]^T$. It is obvious that the performance of $f_1(\theta, \tau)$ massively deteriorates. In addition, we see that $f_2(\theta, \tau)$ shows similar performance to 2D-MUSIC when applied to a "coupling-free" model when the SNR exceeds 25 dB.

VI. CONCLUSION

In this paper, we presented two contributions: The first one (Quadratic Program 1) is an extension to an existing resilient mutual coupling algorithm in order to perform Joint Angle and Delay Estimation (JADE). The second contribution (Quadratic Program 2) is an improvement of the first algorithm, in a sense that we could perform JADE when more antennas suffer from mutual coupling.

ACKNOWLEDGMENT

EURECOM's research is partially supported by its industrial members: ORANGE, BMW Group, SFR, ST Microelectronics, Symantec, SAP, Monaco Telecom, iABG. This work was also supported by RivieraWaves, a CEVA company, and a Cifre scholarship.

REFERENCES

- [1] Stutzman, W.L. Thiele, "G.A. Antenna Theory and Design," 2nd Edition. New York: Wiley, 1998, p. 124-125.
- [2] R. O. Schmidt, "Multiple emitter location and signal parameter estimation," *IEEE Transactions on Antennas and Propagation*, vol. 34, no. 3, pp. 276-280, Mar. 1986.
- [3] R. Roy and T. Kailath, "ESPRIT-Estimation of signal parameters via rotational invariance techniques," *IEEE Transactions on Acoustics, Speech, Signal Processing*, vol.37, no. 7, pp. 984-995, July 1989.
- [4] A. Leshem and M. Wax, "Array Calibration in the Presence of Multipath," *IEEE Transactions on Signal Processing*, 48(1):53-59, Jan 2000.
- [5] J. Pierre and M. Kaveh, "Experimental Performance of Calibration and Direction Finding Algorithms," in *IEEE International Conference on Acoustics, Speech and Signal Processing (ICASSP)*, vol. 2, 1991.
- [6] B. C. Ng and C. M. S. See, "Sensor-array calibration using a Maximum Likelihood approach," *IEEE Trans. Antennas Propag.*, vol. 44, no. 6, pp. 827835, 1996.
- [7] B. Friedlander and A. J. Weiss, "Direction Finding in the Presence of Mutual Coupling," *IEEE Transactions on Antennas and Propagation*, Vol. 39, No. 3, 1991.
- [8] F. Sellone and A. Serra, "A novel online mutual coupling compensation algorithm for uniform and linear arrays," *IEEE Transactions on Signal Processing*, 55, 2, 560-573, 2007.
- [9] M. Pesavento, A. B. Gershman, and K. M. Wong, "Direction finding in partly calibrated sensor arrays composed of multiple subarrays," *IEEE Transactions on Signal Processing*, vol. 50, no. 9, pp. 2103-2115, Sep. 2002.
- [10] C. M. S. See and A. B. Gershman, "Direction-of-arrival estimation in partly calibrated subarray-based sensor arrays," *IEEE Transactions on Signal Processing*, vol. 52, no. 2, pp. 329-338, Feb. 2004.
- [11] B. Liao, Z.G. Zhang, S.C. Chan, "DOA Estimation and Tracking of ULAs with Mutual Coupling," *IEEE Trans. on Aerospace and Electronic Systems*, vol. 48, 891-905, 2012.
- [12] B. Liao and S.-C. Chan, "A cumulant-based method for direction finding in uniform linear array with mutual coupling," *IEEE Antennas and Wireless Propagation Letters*, vol. 13, pp. 1717-1720, 2014.
- [13] J. Dai and Z. Ye, "Spatial smoothing for direction of arrival estimation of coherent signals in the presence of unknown mutual coupling," *IET Signal Process.*, vol. 5, no. 4, pp. 418425, Jul. 2011.
- [14] B. Liao and S. C. Chan, "DOA Estimation of Coherent Signals for Uniform Linear Arrays with Mutual Coupling," *IEEE International Symposium on Circuits and Systems*, Rio de Janeiro, pp. 377-380, 2011.
- [15] J. Dai, W. Xu, D. Zhao, "Real-valued DOA estimation for uniform linear array with unknown mutual coupling," *Elsevier Signal Processing*, Vol. 92, Issue 9, Pages 2056-2065, ISSN 0 165-1684, 2012.
- [16] Ye, Z., *et al.* "DOA estimation for uniform linear array with mutual coupling," *IEEE Transactions on Aerospace and Electronic Systems*, 45, 280288, 2009.
- [17] Ye. Z. and C. Liu, "On the resiliency of MUSIC direction finding against antenna sensor coupling," *IEEE Trans. Antennas and Propagation*, Vol. 56, No. 2, 371380, 2008.
- [18] T. J. Shan, M. Wax, and T. Kailath, "On spatial smoothing for direction of arrival estimation of coherent signals," *IEEE Trans. ASSP*, vol. 33, no.4, pp. 806-811, Apr. 1985.
- [19] A. Bazzi, D. T.M. Slock, L. Meilhac, "Efficient Maximum Likelihood Joint Estimation of Angles and Times of Arrival of Multiple Paths," *IEEE GLOBAL Communications Conference (GLOBECOM), Localization and Tracking : Indoors, Outdoors, and Emerging Networks (LION) Workshop*, December, 2015.
- [20] A. Bazzi, D. T.M. Slock, L. Meilhac, "Single Snapshot Joint Estimation of Angles and Times of Arrival : A 2D Matrix Pencil Approach," *IEEE International Conference on Communications (ICC)*, 2016.
- [21] A. Bazzi, D. T.M. Slock, L. Meilhac, "On Spatio-Frequential Smoothing for Joint Angles and Times of Arrival Estimation of Multipaths," *IEEE International Conference on Acoustics, Speech, and Signal Processing (ICASSP)*, March, 2016.
- [22] M. Wax, T. Kailath, "Detection of Signals by Information Theoretic Criteria," *IEEE Transactions on Acoustics, Speech, and Signal Processing*, VOL. ASSP-3, No. 2, 1985.
- [23] A. Bazzi, D. T.M. Slock, L. Meilhac, "Detection of the number of Superimposed Signals using Modified MDL Criterion : A Random Matrix Approach," *IEEE International Conference on Acoustics, Speech, and Signal Processing (ICASSP)*, 2016.
- [24] P-J Chung, J. F. Bohme, C. F. Mecklenbrauker, and A. Hero, "Detection of the number of signals using the Benjamin Hochberg procedure," *IEEE Trans. on Signal Processing*, 55, 2007.
- [25] R. O. Schmidt, "Multiple emitter location and signal parameter estimation," *IEEE Trans. Antennas and Propagation*, vol. AP-34, pp. 276- 280, 1986.
- [26] M. C. Vanderveen, C. Papadias, and A. Paulraj, "Joint angle and delay estimation (JADE) for multipath signals arriving at an antenna array," *IEEE Commun. Lett.*, vol. 1, no. 1, pp. 1214, 1997.
- [27] A. Bazzi, D. T.M. Slock, L. Meilhac, "Online Angle of Arrival Estimation in the Presence of Mutual Coupling," *IEEE International Workshop on Statistical Signal Processing (SSP)*, 2016.
- [28] A. Bazzi, D. T.M. Slock, L. Meilhac, "On AoA Estimation in the Presence of Mutual Coupling: Algorithms and Performance Analysis," *IEEE Transactions on Signal Processing*, Submitted, 2016.